ACS Macro Letters

Letter

pubs.acs.org/macroletters

Shape Effect of Glyco-Nanoparticles on Macrophage Cellular Uptake and Immune Response

Zhen Li,[†,‡] Liang Sun,[†,§] Yufei Zhang,[‡] Andrew P. Dove,[§] Rachel K. O'Reilly,*[,§] and Guosong Chen*[,‡]

[‡]The State Key Laboratory of Molecular Engineering of Polymers and Department of Macromolecular Science, Fudan University, Shanghai, 200433 China

[§]Department of Chemistry, University of Warwick, Coventry CV4 7AL, United Kingdom

Supporting Information

ABSTRACT: The shells of various poly(DL-lactide)-*b*-poly(acrylic acid) (PDLLA-*b*-PAA) spherical micelles and poly(L-lactide)-*b*-poly(acrylic acid) (PLLA-*b*-PAA) cylindrical micelles were functionalized with mannose to yield glyco-nanoparticles (GNPs) with different shapes and dimensions. All of these GNPs were shown to have good biocompatibility (up to 1 mg/mL). Cellular uptake experiments using RAW 264.7 have shown that the spherical GNPs were internalized to a much greater extent than the cylindrical GNPs and such a phenomenon was attributed to their different endocytosis pathways. It was demonstrated that spherical GNPs were internalized based on clathrin- and caveolin-mediated endocytosis while cylindrical GNPs mainly depended on clathrin-mediated endocytosis. We also found that longer cylindrical GNPs ($L_n \times W_n$ = 215 × 47 nm) can induce an inflammatory response (specifically interleukin 6) more efficiently than shorter cylindrical GNPs ($L_n \times W_n$ = 99 × 50 nm) and spherical GNPs (D_n = 46 nm).

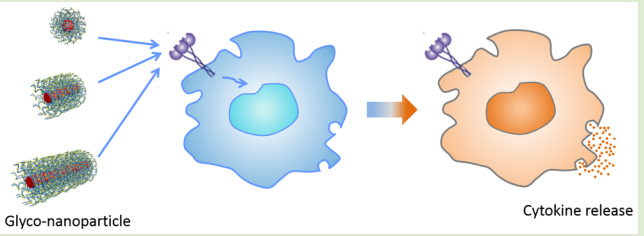

Carbohydrates on the cell surface, known as glycocalyx, are essential mediators of many complex cellular events, including cell adhesion, pathogen invasion, cancer metastasis, immune system activation, and so on.[1] Most of these biological processes involve the specific recognition between carbohydrates and proteins. The individual carbohydrate−protein interaction is generally weak and it is usually compensated by multivalent receptor−ligand presentation in natural systems. This enhanced binding affinity resulting from multiple simultaneous receptor−ligand interactions is called the "cluster glycoside effect" or "multivalent effect".[2]

In recent years, synthetic systems that present carbohydrates in a multivalent form have been extensively developed. For example, glyco-nanoparticles (GNPs) such as glycoliposomes,[3] glycomicelles,[4] glycofullerenes,[5] sugar-functionalized iron oxide nanoparticles,[6] gold nanoparticles,[7] and quantum dots[8] have been fabricated as multivalent scaffolds. Due to their peripheral carbohydrate molecules, GNPs have shown superior biocompatibility and water solubility, and they were designed with various biological functions toward targeted drug delivery,[9] antipathogenic therapy,[5] and cancer vaccine candidates.[10] Among the biological functions of GNPs, the immunological function has received limited study to date. Chiodo and Tefsen et al. have found that galactofuranose functionalized gold nanoparticles could elicit a pro-inflammatory response in dendritic cells, as indicated by the up-regulation of several maturation markers and increased secretion of pro-inflammatory cytokines interleukin 6 (IL-6) and tumor necrosis factor α (TNF-α).[11] In our previous work, we have shown that the spherical GNPs (D_n = 30−40 nm) obtained via a block copolymer self-assembly strategy were able to induce the polarization of mouse primary peritoneal macrophages from immunosuppressive phenotype to inflammatory type.[12]

Both the dimension and the morphology of nanoparticles have been shown to affect the cellular uptake and subsequent protein expression.[13] For example, Chan and co-workers have found that Hela cells internalized more spherical gold nanoparticles (AuNPs; D_n = 14 or 74 nm) than rod-shaped AuNPs ($L_n \times W_n$ = 74 × 14 nm).[14] While Wooley and her colleagues have reported that after conjugation with cell-penetrating peptides, smaller spherical polymeric micelles (D_n = 11 nm) exhibited higher cellular uptake than analogous larger cylindrical micelles ($L_n \times W_n$ = 180 × 20 or 970 × 30 nm).[15] The lower cellular uptake of cylindrical nanoparticles was attributed to the greater membrane wrapping time required for the extended nanoparticles. Very recently, Stenzel's group also explored the cellular uptake behaviors of a number of GNPs with varied morphologies such as cylindrical, flower-like, and raspberry-like GNPs.[16,17]

The size and shape of various nanostructures can also affect the immunological response in biological systems. Niikura et al. have reported that AuNPs of varied shapes coated with West Nile virus envelope (E) protein can induce different cytokine secretion behaviors in dendritic cells: rod-shaped AuNPs ($L_n \times W_n$ = 36 × 10 nm) induced the secretion of the inflammasome-related cytokines interleukin 1β and interleukin 18, while

Received: June 1, 2016
Accepted: August 29, 2016
Published: September 11, 2016

DOI: 10.1021/acsmacrolett.6b00419
ACS Macro Lett. 2016, 5, 1059−1064

spherical (D_n = 19 or 43 nm) or cubic ($L_n \times W_n$ = 41 × 41 nm) AuNPs induce the secretion of the pro-inflammatory cytokines at high levels.[18] More recently, the Caruso group have shown that thiolated poly(methacrylic acid) capsules with different morphologies can influence cytokine secretion by macrophages: short rod-shaped capsules ($L_n \times W_n$ = 720 × 330 nm) provoked a higher increase in TNF-α and interleukin 8 secretion when compared with spherical (D_n = 670 nm) and long rod-shape ($L_n \times W_n$ = 2250 × 305 nm) capsules.[19] These results undoubtedly indicated that the cellular immune response of nanoparticles can be modulated by not just their surface chemistry only, but also by tuning the size and shape of the nanoparticles.

Although most of the studies have explored GNPs with spherical structures, there are a number of reports of GNPs with cylindrical morphologies.[20] More importantly, very few studies have compared the effect of varied dimensions and morphologies of the GNPs on the immunological response. Herein, we explore the effect of the shape of the GNPs on macrophage uptake and subsequent cytokine secretion behavior. Spherical micelles were prepared by direct dissolution of poly(DL-lactide)-*b*-poly(acrylic acid) (PDLLA−PAA) block copolymer in water while cylindrical micelles of varied lengths were obtained using a crystallization-driven self-assembly (CDSA) approach[21,22] of poly(L-lactide)-*b*-poly(acrylic acid) PLLA-*b*-PAA as previously reported.[23] Then the PAA shells of these polymeric micelles were functionalized with mannose, which can specifically bind RAW 264.7 macrophages. When these GNPs were incubated with RAW 264.7 macrophages, spherical GNPs were internalized to a much greater extent than the cylindrical GNPs. This observation was attributed to the different endocytosis pathways of the spherical and cylindrical GNPs. Apart from their different cellular uptake behavior, the inflammatory response was also observed to be affected by the shape of the GNPs. All GNPs enhanced the inflammatory response and promoted a large secretion of TNF-α and monocyte chemotactic protein 1 (MCP-1) to a similar level, but long cylindrical GNPs induced a higher increase of IL-6 than spherical GNPs or short cylindrical GNPs. These results indicate that the size and shape of GNPs play crucial roles in macrophage uptake and immune response and thus can provide a guidance for the further design of GNPs as immunological therapeutic candidates.

The precursors PLLA-*b*-PTHPA and PDLLA-*b*-PTHPA diblock copolymers were achieved using a combination of ring-opening polymerization (ROP) of either L-lactide or DL-lactide and reversible addition−fragmentation chain transfer (RAFT) polymerization of tetrahydropyran acrylate (THPA) monomer from a dual-headed initiator as previously reported.[23] The PLLA-*b*-PTHPA diblock copolymer possessed a hydrophobic weight fraction of 18% which is in the window to access cylindrical morphology according to our previously reported results.[24] ^{1}H nuclear magnetic resonance (NMR) spectroscopic analysis confirmed the successful synthesis of the two diblock copolymers (Figures S3 and S4) while their dispersities ($Đ_M$ < 1.20) were explored using size exclusion chromatography (SEC) analysis (Figures S5 and S6 and Table S1).

To obtain cylindrical nanoparticles, PLLA-*b*-PTHPA was exposed to the previously reported CDSA conditions in a mixture of THF/H_2O (v_{THF}/v_{H_2O} = 20/80).[24] THF was allowed to evaporate during the CDSA. Acetic acid (1 equiv to PTHPA block) was added to promote the hydrolysis of PTHPA into PAA, hence, allowing the formation of amphiphilic block copolymers. The temperature was set at 65 °C, which is above the T_g of polylactide.[25] After 30 h, well-defined PLLA-*b*-PAA cylindrical micelles **3** were obtained. To achieve shorter cylindrical nanoparticles **2**, the ratio between the THF and H_2O in the assembly mixture was adjusted to 5/95, while all the other conditions remained the same. Since less THF (a good solvent for both blocks) in the system will inhibit the PLLA chain folding and the growth of cylindrical micelles during the sphere-to-rod transition, shorter cylindrical micelles were favored.[26] The different lengths of PLLA-*b*-PAA cylinders **1** and **2** were proven using TEM (Figures 1 and S16 and Table 1) and DLS (Figure S17) analyses.

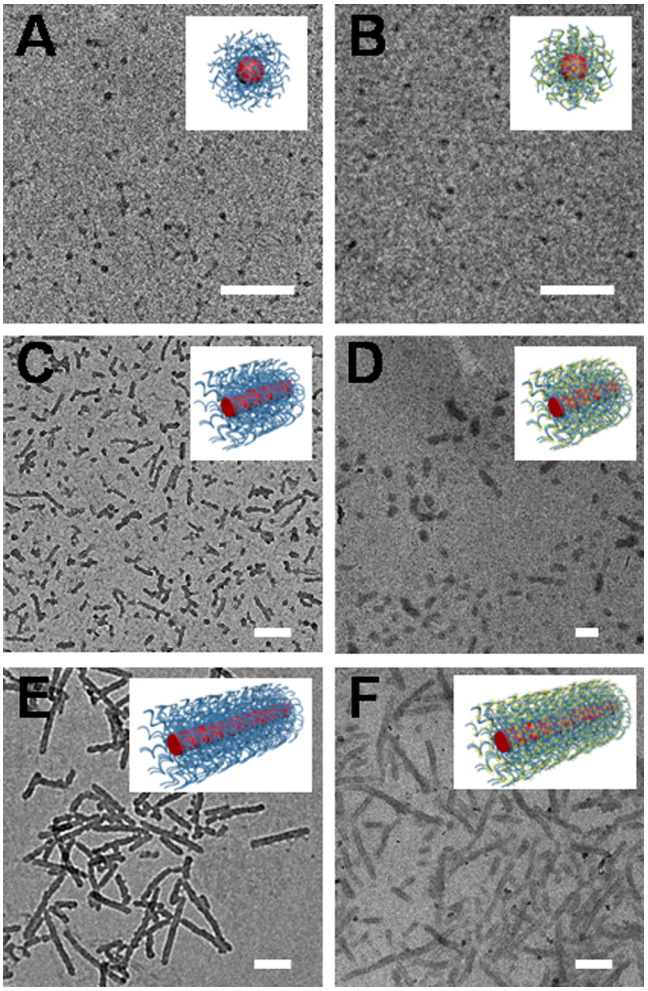

Figure 1. TEM images showing various nanoparticles before (A, C, E) and after (B, D, F) shell functionalization with mannose. (A, B) Spherical micelles **1** and **M1**; (C, D) Short cylindrical micelles **2** and **M2**; (E, F) Long cylindrical micelles **3** and **M3**. TEM samples were air-dried on carbon grids. Scale bar = 200 nm.

Spherical micelles were prepared using the self-assembly of PDLLA-*b*-PTHPA diblock copolymer under a similar condition described above but with a higher composition of THF in the cosolvent (v_{THF}/v_{H_2O} = 40/60). Acetic acid (1 equiv to PTHPA block) was also added to promote the hydrolysis of PTHPA into PAA. The self-assembly was carried out at 65 °C in a sealed vial without evaporation of THF. After 30 h, PDLLA-*b*-

DOI: 10.1021/acsmacrolett.6b00419
ACS Macro Lett. 2016, 5, 1059−1064

Table 1. Characterization Data of PDLLA-*b*-PAA Spherical Micelles and PLLA-*b*-PAA Cylindrical Micelles and Their Corresponding Mannose-Functionalized Nanoparticles

nanoparticle	L_n[a] (nm)	L_w/L_n	D_n[a] (nm)	ζ-potential[b]
sphere **1**			50	−25.4
cylinder **2**	100	1.09	47	−27.7
cylinder **3**	229	1.17	46	−30.6
sphere **M1**			46	−10.9
cylinder **M2**	99	1.10	50	−13.9
cylinder **M3**	215	1.20	47	−13.3

[a]Measured by TEM analysis on stained samples (Figure S16). [b]Measured in 6.7 mM PBS buffer with a concentration of 0.25 mg/mL at 25 °C.

PAA spherical micelles **1** were obtained as confirmed using TEM analysis (Figures 1 and S16).

In order to study the specific interactions between spherical/cylindrical nanoparticles with macrophages, the PAA shells of these self-assembled micelles were modified with amine functionalized mannose (synthetic procedures given in Supporting Information) in H_2O using amidation reactions to yield GNPs **M1**, **M2**, and **M3** (Scheme 1). The compositions of functionalized nanoparticles were confirmed using ^{1}H NMR spectroscopy (Figure S18) with 72, 68, and 73% functionalization ratios of PAA shells, respectively. The zeta potentials of these nanoparticles have all increased to less negative values which proved the successful functionalization of the PAA corona (Table 1). The Concanavalin A (Con A) agglutination assay with GNPs further confirmed that the surfaces of these three nanoparticles were covered with mannose (Figure S22). The dimensions and morphologies of these functionalized nanoparticles remained similar to those before functionalization as determined by TEM (Figures 1 and S16 and Table 1) and DLS (Figure S20) analysis.

The mannose-functionalized GNPs were then fluorescently labeled to enable the study of the cellular uptake. This was achieved through the utilization of similar amidation reactions with 5-aminofluorescein (5-AF) on the various micellar scaffolds (details given in Supporting Information) to give fluorescent spherical GNPs **MF1**, short cylindrical GNPs **MF2**, and long cylindrical GNPs **MF3** (Figures S19 and S21 and Table S2).

As macrophages express a broad range of plasma membrane receptors, they can internalize bound materials in a receptor-mediated way. RAW 264.7, a murine leukemic monocyte macrophage, is known to express moderate mannose receptor CD206,[27] which contains eight extracellular C-type lectin-like domains (CTLD).[28] Binding between individual mannose and single CTLD is weak, with dissociation constants in the millimolar range,[29] but mannose-functionalized GNPs can enhance these weak binding events by multivalent interactions, allowing multiple simultaneous interactions to be made collectively with a multidomain lectin receptor causing a much stronger association.[30]

Scheme 1. Preparation of PDLLA-*b*-PAA Spherical Micelles 1, PLLA-*b*-PAA Cylindrical Micelles 2 and 3, and Their Shell Functionalizations with Mannose to Afford GNPs M1−M3

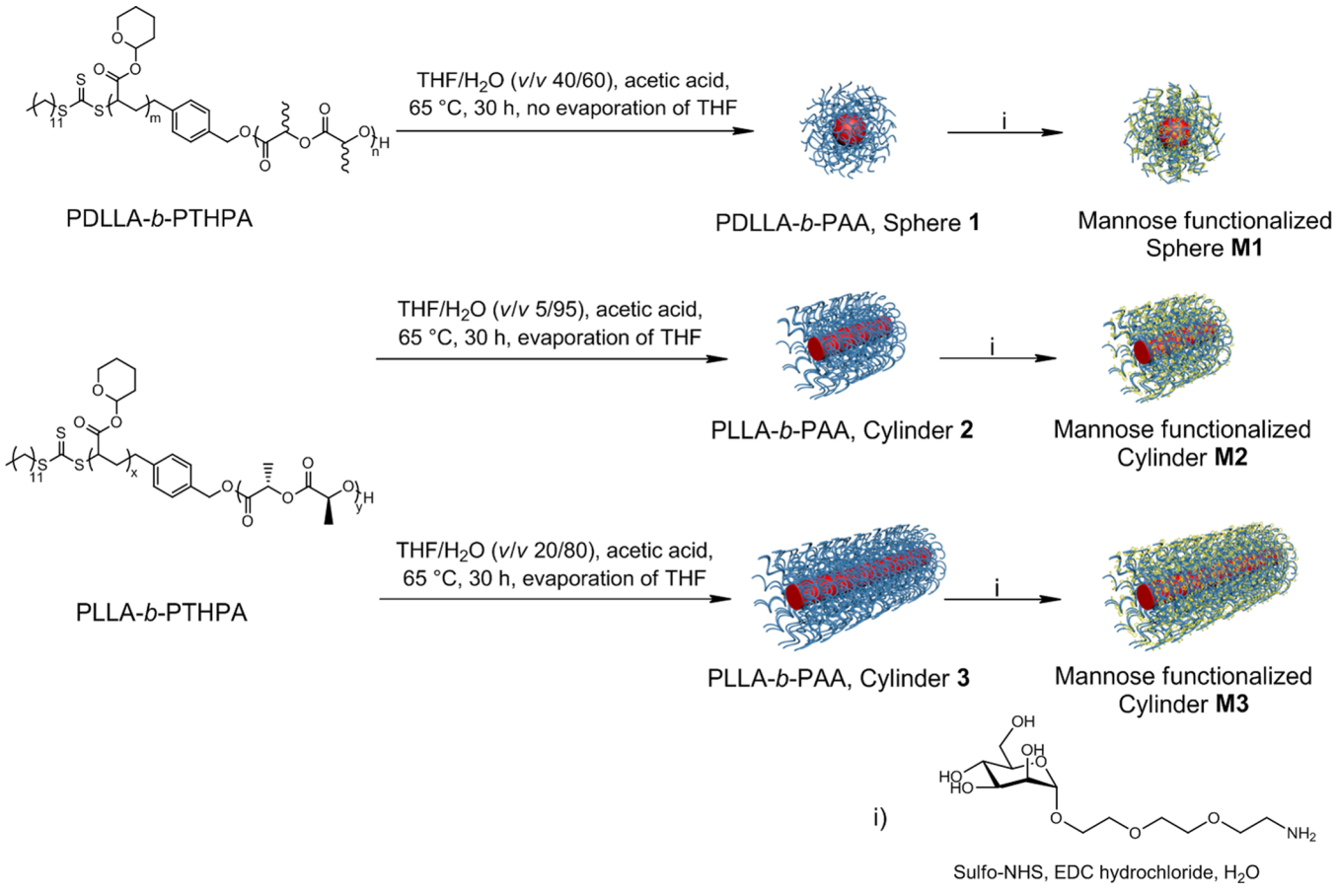

DOI: 10.1021/acsmacrolett.6b00419
ACS Macro Lett. 2016, 5, 1059−1064

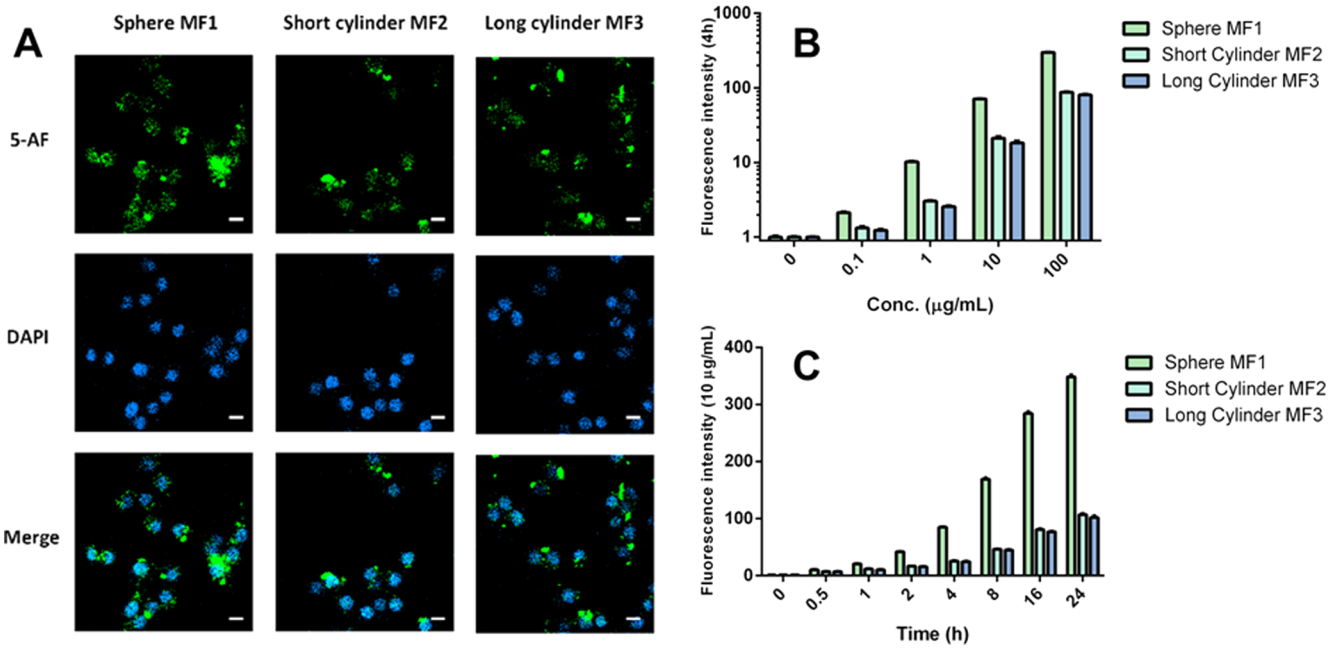

Figure 2. (A) Confocal fluorescence microscopy images showing the internalization of various GNPs by macrophages after 4 h of incubation (concentration = 20 μg/mL). Scale bar = 10 μm. Graphs showing dose dependence (B) and time dependence (C) of the binding of GNPs with RAW 264.7 macrophages.

Prior to performing the endocytosis experiments, the evaluation on the cytotoxicity of various GNPs was explored as it is of particular importance since cell death due to the toxicity of GNPs may lead to incorrect results regarding the interplay between the shape/size of GNPs and the cellular uptake. All GNPs showed no obvious cytotoxicity below 1 mg/mL, which confirmed their good biocompatibility (Figure S24). The fluorescence intensity was used to represent the amount of the particles internalized in the cellular uptake studies. In order to quantitatively compare the amount of endocytosis between different GNPs, the fluorescence intensities of GNPs were first normalized. Short cylindrical micelles **MF2** and long cylindrical micelles **MF3** were found to exhibit similar fluorescence intensities, while spherical micelles **MF1** possessed higher fluorescence intensity at the same concentration (1 mg/mL; Figure S23). Since the same equivalent amount of 5-AF (0.03 equiv to PAA) was used to functionalize the PAA shell of various nanoparticles, the difference of fluorescence intensity between spheres and cylinders is most likely due to the different environment of the 5-AF chromophore. Spherical micelles possess a higher interfacial curvature with a less crowded shell than cylindrical micelles,[31] thus, the 5-AF at the shell of spherical micelles may have less opportunity to undergo self-quenching and, hence, would be expected to show a higher fluorescence intensity. Therefore, to achieve a similar fluorescence intensity as those of cylindrical micelles **MF2** and **MF3**, fluorescent spherical micelles **MF1** were diluted using the nonfluorescent spherical micelles **M1** before cellular uptake experiments (Figure S23).

Confocal microscopy was used to investigate the macrophage uptake process of various fluorescent GNPs. After the GNPs (20 μg/mL) were incubated with macrophages for 4 h, the internalization of **MF1**, **MF2**, and **MF3** by macrophages were clearly observed (Figure 2A). The quantitative study of macrophage uptake of different GNPs was performed using flow cytometry. In dose dependency experiments (Figure 2B), an appropriate amount of cells were cultured in medium containing different amounts of GNPs at a fixed incubation time of 4 h. It was found that greater amounts of the smaller spherical micelles **MF1** were internalized than that of the short cylindrical **MF2** and the long cylindrical **MF3**, although the difference in uptake between the long and short cylindrical micelles was negligible. When the concentration of GNPs was fixed at 10 μg/mL, the time dependency experiment revealed a gradual increase of GNPs' endocytosis extent as the incubation time was increased (Figure 2C). Both the dose and time dependency experiments proved that many more spherical GNPs were internalized than cylindrical GNPs.

It is well-known that the extracellular substances can be transported into cells through several different pathways: phagocytosis, macropinocytosis, clathrin-dependent endocytosis, and caveolin-dependent endocytosis.[32] The endocytosis pathways of these three GNPs were also investigated. To determine the uptake mechanisms of various GNPs, specific inhibitors were selected to treat the cells before incubation with different GNPs: rottlerin was used to inhibit macropinocytosis,[33] chloropromazine was utilized to inhibit clathrin-mediated endocytosis,[34] while genistein was chosen to inhibit the caveolin-mediated endocytosis pathway.[35] As shown in Figure 3, the cellular uptake efficiency of spherical micelles **MF1** decreased dramatically after pretreatment of chloropromazine or genistein, which indicated that the spherical micelles **MF1** were internalized by clathrin- and caveolin-mediated endocytosis. The cellular uptake efficiency of short cylindrical micelles **MF2** and long cylindrical micelles **MF3** decreased significantly only after the pretreatment of chloropromazine, indicating that the cylindrical GNPs were mainly internalized by clathrin-mediated endocytosis regardless of the length of the cylinder. The difference of the endocytosis pathway could be the reason why greater amounts of spherical GNPs were internalized than the cylindrical GNPs.

DOI: 10.1021/acsmacrolett.6b00419
ACS Macro Lett. 2016, 5, 1059−1064

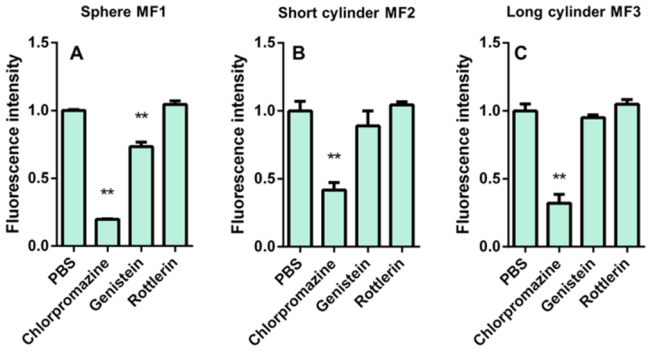

Figure 3. Inhibition tests of (A) spherical GNPs **MF1**, (B) short cylindrical GNPs **MF2**, and (C) long cylindrical GNPs **MF3**. Data are expressed as the mean ± SEM of three independent experiments; $*p < 0.05$ and $**p < 0.01$.

Macrophages are scavengers of the immune system. After internalizing external molecules/materials, macrophages can be activated to secrete cytokines and chemokines. These mediators were released in a tightly orchestrated manner to regulate the progression of an inflammatory response.[36] Several botanical polysaccharides have been used to modulate macrophage immune function, and this macrophage activation by polysaccharide is considered to be mediated through the specific binding between carbohydrates and receptors.[37] However, the activation of polysaccharide from natural source suffers from batch-to-batch variations. Similar to natural polysaccharides, GNPs can also be used for macrophage immunomodulation as therapeutic potential and showed better structural adjustability.[11,12] Besides, previous studies have shown that the shape of nanoparticles also influenced cytokine secretion.[18,38,39]

Hence, we sought to examine the shape effect of different GNPs on their macrophage activation abilities. RAW 264.7 macrophages were incubated with various GNPs for 24 h and the cytokines secretion were analyzed using enzyme-linked immunosorbent assay (ELISA). Three characteristic cytokines to inflammatory cells, that is, IL-6, TNF-α, and MCP-1 were evaluated. As shown in Figure 4, all the GNPs stimulated higher secretion of the inflammatory cytokines compared to the control group. However, it is notable that spherical GNPs **M1** promoted a stronger increase of IL-6 than short cylindrical GNPs **M2**, while long cylindrical GNPs **M3** promoted a stronger improvement of IL-6 than spherical GNPs. For the other two cytokines, no significant difference in secretion was observed among the three GNPs. This result of differing IL-6 secretion based on differing morphologies is very interesting. Considering the endocytosis results, we hypothesized that individual cylindrical GNPs can induce the inflammatory response more efficiently than individual spherical GNPs, and there is an interplay between number and efficiency of GNPs due to the larger endocytosis degree observed for spherical particles. To confirm this hypothesis, the same experiment was performed but the dosage of spherical GNPs was decreased from 10 μg/mL to 2 μg/mL, so that spherical GNPs and cylindrical GNPs would have a similar degree of endocytosis. It was found that long cylindrical micelles **M3** promoted a higher increase of IL-6 than short cylindrical micelles **M2** and spherical micelles **M1** (Figure S25), which is in accordance with our expectation. However, given that the signaling pathways involved in macrophage activation are relatively complex, the exact mechanism for the effect of the GNPs' shape on cytokine secretion could not be elucidated and requires more detailed investigations.

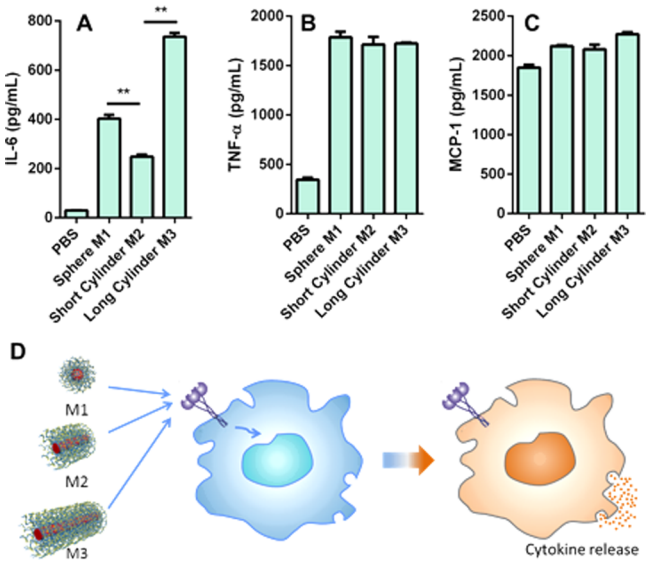

Figure 4. GNPs (10 μg/mL) promoted the (A) IL-6, (B) TNF-α, and (C) MCP-1 secretions of macrophages after 24 h incubation measured by ELISA. Data are expressed as the mean ± SEM of three independent experiments; $*p < 0.05$ and $**p < 0.01$. (D) Schematic illustration of the shape effect of GNPs on cytokine secretion of macrophage cells.

In conclusion, we have functionalized the shells of PDLLA-*b*-PAA spherical micelles and PLLA-*b*-PAA cylindrical micelles with mannose without affecting their morphologies. The cellular uptake and immune response of these GNPs were then explored. It was found that spherical GNPs were internalized more by RAW 264.7 macrophages than cylindrical GNPs. The difference of the endocytosis pathways between spherical and cylindrical GNPs could explain this observation: spherical GNPs were internalized based on clathrin- and caveolin-mediated endocytosis while cylindrical GNPs mainly depended on clathrin-mediated endocytosis. It is also worth noting that longer cylindrical GNPs can induce the inflammatory response (IL-6) more efficiently than shorter cylindrical GNPs and spherical GNPs. These results can provide us with the guidance of the development of new GNPs toward immunological therapeutic candidates.

■ ASSOCIATED CONTENT

Supporting Information

The Supporting Information is available free of charge on the ACS Publications website at DOI: 10.1021/acsmacrolett.6b00419.

Synthetic details and characterization data of polymers, amine-functionalized mannose, and various GNPs (PDF).

■ AUTHOR INFORMATION

Corresponding Authors

*E-mail: rachel.oreilly@warwick.ac.uk.
*E-mail: guosong@fudan.edu.cn.

Author Contributions

†These authors contributed equally (Z.L. and L.S.).

DOI: 10.1021/acsmacrolett.6b00419
ACS Macro Lett. 2016, 5, 1059−1064

Notes

The authors declare no competing financial interest.

■ ACKNOWLEDGMENTS

National Natural Science Foundation of China (Nos. 91527305, 21474020, 91227203, 5141101211, and 51322306) is acknowledged for financial support. The EPSRC, The Royal Society, and ERC are acknowledged for funding.

■ REFERENCES

(1) Varki, A.; Cummings, R.; Esko, J.; Freeze, H.; Hart, G.; Marth, J. *Essentials of Glycobiology*, 2nd ed.; Cold Spring Harbor: NY, 2009.
(2) Lundquist, J. J.; Toone, E. J. *Chem. Rev.* **2002**, *102*, 555.
(3) DeFrees, S. A.; Phillips, L.; Guo, L.; Zalipsky, S. *J. Am. Chem. Soc.* **1996**, *118*, 6101.
(4) Babiuch, K.; Dag, A.; Zhao, J.; Lu, H.; Stenzel, M. H. *Biomacromolecules* **2015**, *16*, 1948.
(5) Munoz, A.; Sigwalt, D.; Illescas, B. M.; Luczkowiak, J.; Rodriguez-Perez, L.; Nierengarten, I.; Holler, M.; Remy, J.-S.; Buffet, K.; Vincent, S. P.; Rojo, J.; Delgado, R.; Nierengarten, J.-F.; Martin, N. *Nat. Chem.* **2015**, *8*, 50.
(6) Basuki, J. S.; Esser, L.; Duong, H. T. T.; Zhang, Q.; Wilson, P.; Whittaker, M. R.; Haddleton, D. M.; Boyer, C.; Davis, T. P. *Chem. Sci.* **2014**, *5*, 715.
(7) Barrientos, Á. G.; de la Fuente, J. M.; Rojas, T. C.; Fernández, A.; Penadés, S. *Chem. Eur. J.* **2003**, *9*, 1909.
(8) Kikkeri, R.; Laurino, P.; Odedra, A.; Seeberger, P. H. *Angew. Chem., Int. Ed.* **2010**, *49*, 2054.
(9) Lai, C.-H.; Chang, T.-C.; Chuang, Y.-J.; Tzou, D.-L.; Lin, C.-C. *Bioconjugate Chem.* **2013**, *24*, 1698.
(10) Parry, A. L.; Clemson, N. A.; Ellis, J.; Bernhard, S. S. R.; Davis, B. G.; Cameron, N. R. *J. Am. Chem. Soc.* **2013**, *135*, 9362.
(11) Chiodo, F.; Marradi, M.; Park, J.; Ram, A. F. J.; Penadés, S.; van Die, I.; Tefsen, B. *ACS Chem. Biol.* **2014**, *9*, 383.
(12) Su, L.; Zhang, W.; Wu, X.; Zhang, Y.; Chen, X.; Liu, G.; Chen, G.; Jiang, M. *Small* **2015**, *11*, 4191.
(13) Verma, A.; Stellacci, F. *Small* **2010**, *6*, 12.
(14) Chithrani, B. D.; Ghazani, A. A.; Chan, W. C. W. *Nano Lett.* **2006**, *6*, 662.
(15) Zhang, K.; Fang, H.; Chen, Z.; Taylor, J.-S. A.; Wooley, K. L. *Bioconjugate Chem.* **2008**, *19*, 1880.
(16) Dag, A.; Zhao, J. C.; Stenzel, M. H. *ACS Macro Lett.* **2015**, *4*, 579.
(17) Dag, A.; Lu, H. X.; Stenzel, M. *Polym. Chem.* **2015**, *6*, 7812.
(18) Niikura, K.; Matsunaga, T.; Suzuki, T.; Kobayashi, S.; Yamaguchi, H.; Orba, Y.; Kawaguchi, A.; Hasegawa, H.; Kajino, K.; Ninomiya, T.; Ijiro, K.; Sawa, H. *ACS Nano* **2013**, *7*, 3926.
(19) Chen, X.; Yan, Y.; Müllner, M.; Ping, Y.; Cui, J.; Kempe, K.; Cortez-Jugo, C.; Caruso, F. *Biomacromolecules* **2016**, *17*, 1205.
(20) Hong, S. Y.; Tobias, G.; Al-Jamal, K. T.; Ballesteros, B.; Ali-Boucetta, H.; Lozano-Perez, S.; Nellist, P. D.; Sim, R. B.; Finucane, C.; Mather, S. J.; Green, M. L. H.; Kostarelos, K.; Davis, B. G. *Nat. Mater.* **2010**, *9*, 485.
(21) Gadt, T.; Ieong, N. S.; Cambridge, G.; Winnik, M. A.; Manners, I. *Nat. Mater.* **2009**, *8*, 144.
(22) Gilroy, J. B.; Gadt, T.; Whittell, G. R.; Chabanne, L.; Mitchels, J. M.; Richardson, R. M.; Winnik, M. A.; Manners, I. *Nat. Chem.* **2010**, *2*, 566.
(23) Petzetakis, N.; Dove, A. P.; O'Reilly, R. K. *Chem. Sci.* **2011**, *2*, 955.
(24) Sun, L.; Petzetakis, N.; Pitto-Barry, A.; Schiller, T. L.; Kirby, N.; Keddie, D. J.; Boyd, B. J.; O Reilly, R. K.; Dove, A. P. *Macromolecules* **2013**, *46*, 9074.
(25) Becker, J. M.; Pounder, R. J.; Dove, A. P. *Macromol. Rapid Commun.* **2010**, *31*, 1923.
(26) Petzetakis, N.; Walker, D.; Dove, A. P.; O'Reilly, R. K. *Soft Matter* **2012**, *8*, 7408.
(27) Stahl, P. D.; Rodman, J. S.; Miller, M. J.; Schlesinger, P. H. *Proc. Natl. Acad. Sci. U. S. A.* **1978**, *75*, 1399.
(28) Taylor, P. R.; Martinez-Pomares, L.; Stacey, M.; Lin, H.-H.; Brown, G. D.; Gordon, S. *Annu. Rev. Immunol.* **2005**, *23*, 901.
(29) Lee, R. T.; Ichikawa, Y.; Kawasaki, T.; Drickamer, K.; Lee, Y. C. *Arch. Biochem. Biophys.* **1992**, *299*, 129.
(30) Mammen, M.; Choi, S. K.; Whitesides, G. M. *Angew. Chem., Int. Ed.* **1998**, *37*, 2754.
(31) Blanazs, A.; Armes, S. P.; Ryan, A. J. *Macromol. Rapid Commun.* **2009**, *30*, 267.
(32) Mayor, S.; Pagano, R. E. *Nat. Rev. Mol. Cell Biol.* **2007**, *8*, 603.
(33) Sarkar, K.; Kruhlak, M. J.; Erlandsen, S. L.; Shaw, S. *Immunology* **2005**, *116*, 513.
(34) Rejman, J.; Bragonzi, A.; Conese, M. *Mol. Ther.* **2005**, *12*, 468.
(35) Mundy, D. I.; Li, W. P.; Luby-Phelps, K.; Anderson, R. G. W. *Mol. Biol. Cell* **2012**, *23*, 864.
(36) Janeway, C. A.; Medzhitov, R. *Annu. Rev. Immunol.* **2002**, *20*, 197.
(37) Schepetkin, I. A.; Quinn, M. T. *Int. Immunopharmacol.* **2006**, *6*, 317.
(38) Hutter, E.; Boridy, S.; Labrecque, S.; Lalancette-Hébert, M.; Kriz, J.; Winnik, F. o. M.; Maysinger, D. *ACS Nano* **2010**, *4*, 2595.
(39) Sun, B.; Ji, Z.; Liao, Y.-P.; Wang, M.; Wang, X.; Dong, J.; Chang, C. H.; Li, R.; Zhang, H.; Nel, A. E.; Xia, T. *ACS Nano* **2013**, *7*, 10834.

DOI: 10.1021/acsmacrolett.6b00419
ACS Macro Lett. 2016, 5, 1059−1064